

19th CIRP Conference on Modeling of Machining Operations

# Modeling the effect of workpiece temperature on micromagnetic high-speed-3MA-testing in case of AISI 4140

Alpcan Güray<sup>a,\*</sup>, David Böttger<sup>b</sup>, Germán González<sup>a</sup>, Florian Stamer<sup>a</sup>,  
Gisela Lanza<sup>a</sup>, Bernd Wolter<sup>b</sup>, Volker Schulze<sup>a</sup>

<sup>a</sup>wbk Institute of Production Science, Karlsruhe Institute of Technology (KIT), Kaiserstr. 12, 76131 Karlsruhe, Germany

<sup>b</sup>Fraunhofer Institute for Nondestructive Testing (IZFP), Campus E3 1, 66123 Saarbrücken, Germany

\* Corresponding author. Tel.: +49-721-608-42455; fax: +49-721-608-45004. E-mail address: [alpcan.gueray@kit.edu](mailto:alpcan.gueray@kit.edu)

## Abstract

The growing trend towards industry 4.0 requires in-process identification of the surface properties. The non-destructive highspeed-3MA-testing can be used to characterize surface layers of ferrous materials during turning processes. However, in-process measurements will result in higher workpiece temperatures and thus would interfere with the micromagnetic properties of the workpiece. In the presented study, workpiece surface temperatures will be experimentally determined when turning AISI 4140. Further on, workpieces will be heated up to the respective temperatures, which will then be measured with the 3MA-sensor as they rotate. The effect of temperature will be modelled and used for compensating the associated errors.

© 2023 The Authors. Published by Elsevier B.V.

This is an open access article under the CC BY-NC-ND license (<https://creativecommons.org/licenses/by-nc-nd/4.0>)

Peer review under the responsibility of the scientific committee of the 19th CIRP Conference on Modeling of Machining Operations

*Keywords:* Eddy Current; Turning; White layers; 3MA, Surface Integrity

## 1. Introduction

During a machining operation the workpiece surface is subjected to mechanical and thermal stresses, which subsequently may change its surface properties, e.g. hardness and residual stresses [1]. Resulting new surface properties can increase or decrease workpiece's fatigue resistance and therefore its lifespan [2].

When machining ferrous metals, nickel and titanium alloys thermomechanical loading of the surface can induce so-called white layers (WL) at workpiece subsurface [3]. The microstructure of WL depend on the dominant load (thermal or mechanical) and its thickness is governed by tool wear, cutting speed and feed rate [4–6]. In case of AISI 4140, full martensitic or martensitic-retained-austenitic WL have about 25% higher hardness than the quenched material and can result in tensile residual stresses causing a brittle surface and low fatigue life [3].

Nowadays, the use of thin-film sensors [7], Micromagnetic Multiparameter Micro-structure and Stress Analyzer (3MA) [8] and dynamometers [9] allows in-process measurement of tool temperature, wear and process forces. The valuable data generated by the respective sensors allows modelling of surface integrity and thus in-process control of machining. The capabilities of the 3MA-testing are proven in several applications, ranging from component testing in nuclear power plants against material degradation to grinding induced burns [10].

Currently, an active research topic is to use in-process 3MA-testing and closed loop control when turning AISI 4140 to eliminate WL, ensuring the quality of the workpiece and prolonging its lifespan [1]. During machining, the workpiece temperature increases due to the plastic deformation of the material and the friction between the tool and workpiece [11]. As an increase in workpiece temperature would change the electromagnetic properties of metals [12], the increased

workpiece temperature during machining would have an impact on 3MA-measurements [13,14].

In the presented work, the effect of temperature on high-speed-3MA measurement of AISI 4140 components was determined. First, AISI 4140 specimens will be rotated and heated up to the experimentally determined achievable surface temperatures during turning, and their respective micromagnetic properties will be measured by high-speed-3MA. Afterwards, by using Pearson correlation, temperature dependent 3MA-parameters will be determined and modeled. Finally, the models will be used to reverse the effect of temperature on 3MA-parameters, compensating the measurement error caused by temperature.

## 2. State of the art

An in-process, direct measurement of the WL and its thickness is currently not possible as it would require laboratory investigation on polished and etched samples to make them visible, which would interrupt the machining process. However, the use of soft-sensors allows in-process indirect identification of the WL, microstructure and surface integrity [15,16,9].

Micromagnetic non-destructive testing is suitable for measurement of material properties and allows mechanical and microstructural characterization of ferromagnetic materials. Contactless in-process micromagnetic testing enables process monitoring and material behavior. However, different challenges caused by probe-head lift-off variations, measurement frequency and temperature behavior of the micromagnetic properties need to be addressed [8]. Temperature dependencies for carbon steel and its effect on magnetic Barkhausen noise has been previously addressed by researchers [13,14].

3MA-tests measure numerous electromagnetic properties, by utilizing multi-frequency eddy current analysis, harmonic analysis of the tangential magnetic field strength, incremental permeability and Barkhausen noise. The depth of analysis is limited due to the skin effect and depends on the applied magnetic field strength, excitation frequency and the design of the measurement equipment as well as the investigated specimen shape and size. Furthermore, a calibration is mandatory to determine a mathematical model to correlate a target quantity with the micromagnetic parameters. [10]

The appearance of WL and its corresponding microstructure, hardness and stresses can be measured with micromagnetic techniques although a separation of the mentioned influencing factors is challenging [8]. For the in-process indirect measurement of WL no other than micromagnetic techniques are favorable, due to its speed and simple use. On the one hand, several specific micromagnetic values based on coercive field strength “Hc” [8] or remanence “Br” [15] can be directly correlated with hardness, residual stresses and retained austenite content in AISI 4140. On the other hand, non-linear behavior of specific values due to anisotropy in the material can be often observed. Therefore, a combination of the different techniques in one system like 3MA for robust calibration and identification can be favorable [10].

## 3. Experimental setup

In order to find the effect of workpiece temperature on 3MA-measurements, turning experiments were conducted. Later, machined specimens were heated up and measured by a high-speed-3MA head while being rotated in lathe.

### 3.1. Measurement of workpiece temperature during turning

During a turning operation the workpiece temperature increases due to the plastic deformation of the material in the primary shear zone and the friction between the tool and workpiece. To determine the workpiece temperature, dry longitudinal turning experiments were conducted with an Index G200 CNC turning machine. The workpiece material was AISI 4140 steel which was tempered at 650°C. During all 9 experiments the same TiCN-coated carbide insert was used and tool wear was inspected after each experiment. The cutting parameters and the insert geometry have been documented in Table 1. Where  $v_c$  denotes the cutting speed,  $f$  the feed rate,  $a_p$  the depth of cut,  $\alpha$  the clearance angle,  $\gamma$  the rake angle,  $\kappa$  the principal cutting edge angle,  $\lambda$  the inclination angle of the cutting edge, and  $r_e$  the corner radius of the insert. Experiments using highest feed rate together with the cutting speed were not carried on as the flying chips interfered with the measurements.

Table 1. Cutting parameters and insert geometry for temperature measurements

$v_c$	$f$	$a_p$	$\alpha$	$\gamma$	$\kappa$	$\lambda$	$r_e$
m/min	mm/rev	mm	°	°	°	°	mm
100, 300	0.05, 0.3	0.2, 0.5, 1	7	0	95	0	0.4

Workpiece surface temperature was captured using an Infratech ImageIR 5385 S highspeed infrared camera and a macro lens which is capable of measuring temperatures between -40 to 1200°C. Using the camera and macro lens each pixel was able to capture the temperature at a 150x150  $\mu\text{m}$  area with  $\pm 1^\circ\text{C}$  error. The experimental setup has been illustrated on Fig. 1. The tool engagement point and the measurement point are separated by 215° causing the heat from the surface to penetrate into the workpiece, cooling down the workpiece surface.

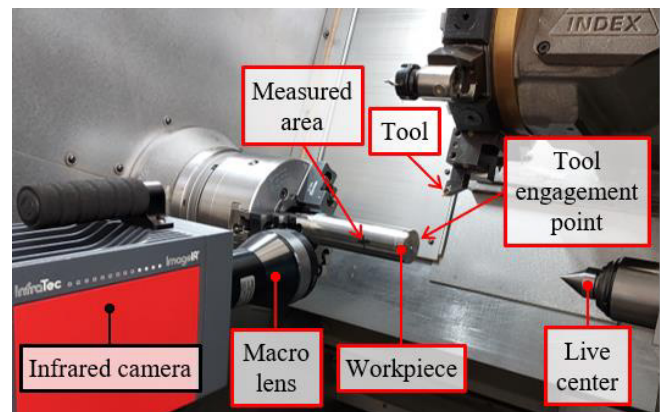


Fig. 1. Experimental setup for the temperature measurements

### 3.2. 3MA-testing of heated specimens

In order to quantify the effect of workpiece temperature on the high-speed-3MA sensor, three previously machined specimens were measured while being rotated at 300 RPM. Specimens were heat treated according to DIN10083 and were tempered ( $T_{Temp}$ ) at 300°C, 450°C and 600°C, respectively. Each specimen was divided into 17 sections (see Fig. 2) and each section was dry turned under different cutting conditions, as presented in Table 2. The cutting insert is the same type, which was used in Section 3.1. Experiments using the combination of a feed rate,  $f = 0.3$  mm/rev with cutting speed,  $v_c = 300$  m/min were not conducted.

Table 2. Cutting parameters used for the specimens

$v_c$	$f$	$a_p$	$T_{Temp}$
m/min	mm/rev	mm	°C
100, 200, 300	0.05, 0.1, 0.15, 0.2, 0.25, 0.3	0.2	300, 450, 600

All specimens were left in an oven to heat up to 100 °C. Because, after installing the specimens to the lathe chuck workpiece surface temperatures were 90 °C. A lift-off of 50  $\mu$ m was set between the workpiece and the 3MA-head. For each specimen 17 consecutive high-speed-3MA tests were conducted from front until the end section. Temperature measurements were done before the first and after last section with Type K thermocouple which has a measurement error of  $\pm 2.5$  °C. As the specimens cooled to 67 °C after 17 consecutive measurements, 3MA-tests were conducted from end section to the front section (with only 90 °C start temperature). Fig. 2 shows the experimental setup used for the high-speed-3MA tests.

All 3 specimens were measured with the 3MA sensor at ambient room temperature (24 °C) before and after heating, to ensure no microstructural changes were caused by heating. Also, all specimens were measured with 67 °C and 45 °C initial temperatures to cover a broad range of temperature spectrum.

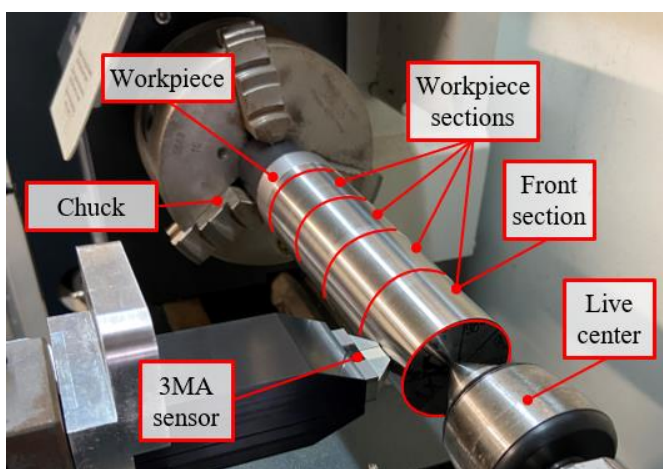


Fig. 2. Experimental setup used for 3MA testing of heated specimens

### 4. Cooling Simulations

As the specimens tested in Section 3.2 cooled rapidly during the experiment, temperature measurements were not done between sections to keep the specimens warm. However, this results in indefinite section temperatures during high-speed-3MA measurements. To find out the temperature of respective sections, transient-state thermal simulations were conducted in FEM Software, ANSYS ®.

A cylinder with 47 mm diameter and 100 mm length was modelled and meshed with 2016 hexahedron elements with a homogenous initial temperature of 100 °C. Temperature dependent thermal conductivity and specific heat capacity coefficients of AISI 4140 steel (tempered at 650 °C) were used from ANSYS database and were 43.25 W/(m·K) and 445 J/(kg·K) at the simulated temperature range.

Convection and radiation of heat were allowed from all cylinder surfaces. Due to the reflective specimen surface an emissivity of 0.275 was set, which is between the emissivity of polished and rolled steel surface. A convective heat transfer coefficient of  $h = 28$  W/(m<sup>2</sup>·K) was found by calibrating the simulation model with temperature measurements done before and after a 3MA measurement. As the lathe was stopped to move the 3MA-sensor between sections, the used heat transfer coefficient is a result of free and forced convection. In Fig. 3 the simulated workpiece surface temperature and the measured workpiece surface temperatures are plotted vs. time.

The heat transfer coefficient calibration was done by using a pair of time stamps provided by the 3MA-data and temperature measurements before the first and after the last section of the respective specimen. The mean absolute error between the simulated and experimental measurements were 1.3 °C, the maximum error between the simulation and the experimental measurement was 8 °C. Presented errors are caused by measurement errors of the thermo couple, the delay between the last 3MA-test and the temperature measurement and the associated calibration error.

Overall the temperature drops between the first and last sections were simulated accurately. Therefore, simulated temperatures are further used to assign surface temperature values at the time of the 3MA measurement.

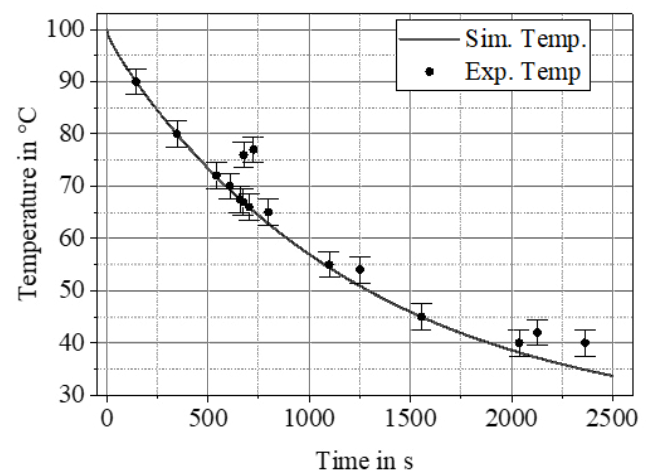


Fig. 3. Simulated and experimental temperatures vs. time

## 5. Results and discussion

### 5.1. Workpiece surface temperature during AISI 4140 turning

To find the surface temperatures when turning AISI 4140, experiments were conducted according to Section 3.1. At the following Fig. 4 captured thermal images under varying depth of cut have been presented where constant cutting speed,  $v_c = 300$  m/min and feed,  $f = 0.05$  mm were used.

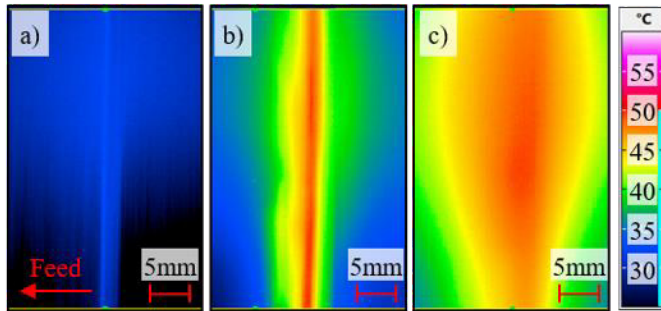


Fig. 4. Thermal images during (a)  $a_p = 0.2$ ; (b)  $a_p = 0.5$ ; (c)  $a_p = 1$  mm

As can be seen in Fig. 4 workpiece surface temperatures increase with an increasing depth of cut and the heat is quickly dissipated to the workpiece. As the high-speed-3MA measurements take place in an area of  $4 \times 4$  mm, the dissipated heat would have an impact during in-process 3MA-measurements since the intensely warmed up area during turning is wider than 4 mm (see Fig 4).

In Fig. 5, maximum temperatures captured during respective turning operations have been illustrated. An increase in all 3 examined cutting parameters resulted in increased temperatures due to the increased material removal rate where, the depth of cut had the greatest influence on workpiece surface temperature. A possible explanation for this is (linearly) increasing shear plane width at the primary deformation zone which would increase the dissipated heat to the workpiece. At the used experimental settings, higher depth of cut  $a_p$  linearly increases contact area to the neighboring material. Hence, enabling heat flow and preheating the neighboring material which, will be removed in the consecutive cut.

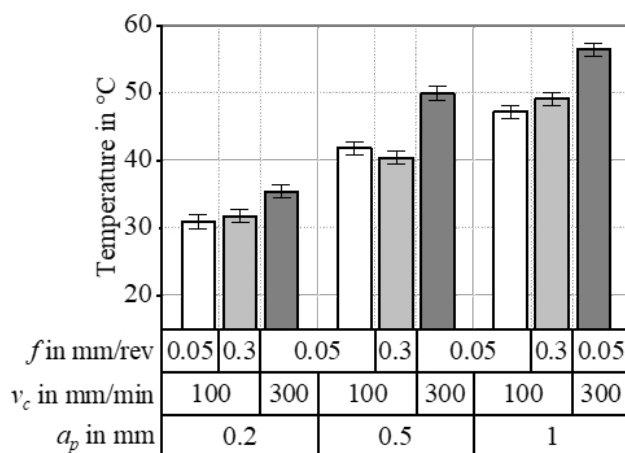


Fig. 5. Maximum temperatures captured by the infrared camera

The cutting speed and feed rate had lesser impact on the surface temperatures when compared to impact of depth of cut. As increased cutting speeds cause higher temperatures at the shear plane, which in turn increase the workpiece surface temperature. However, much of the heat is transported away from the workpiece with chips, resulting in minor temperature increase at the final surface. In case of an increased feed rate, the shear plane length increases, which causes proportional increase of heat generation in the shear plane. However, much of the heat is again transported away resulting in a minor increase of temperature at the final workpiece surface. Kronenberg's research presented similar results, where the percentage of heat transport by chips increased non-linearly from 69 % to 75 % when the cutting speed was increased from 20 to 60 m/min [17].

### 5.2. Effect of temperature on high-speed-3MA-testing

To find and compensate the effect of workpiece temperature on 3MA-testing, measurements were done on 3 different heated specimens with 5 different initial temperatures, as described in Section 3.2. Where, each specimen had a different tempering level and each segment (17 segments) was machined under different machining conditions. In total 255 3MA-tests were done, where the measured surfaces presented 51 unique surface properties, due to the different machining and tempering conditions.

A single 3MA-measurement results in 41 different sensor output by analyzing electromagnetic properties of the specimen with 4 different methods. Since the measured specimens have different microstructure and surface properties, the 3MA-measurements vary at room temperature and at elevated temperatures. This poses a challenge to understand the influence of temperature on 3MA-measurements. To overcome this problem, measurements done at respective segments under varying temperatures have been normalized by subtracting all sensor data from the sensor data measured at room temperature. The data points before and after normalization can be seen in Fig 6. This procedure allows us to disregard the effect of the initial microstructure on the respective 3MA sensor output at room and elevated temperatures.

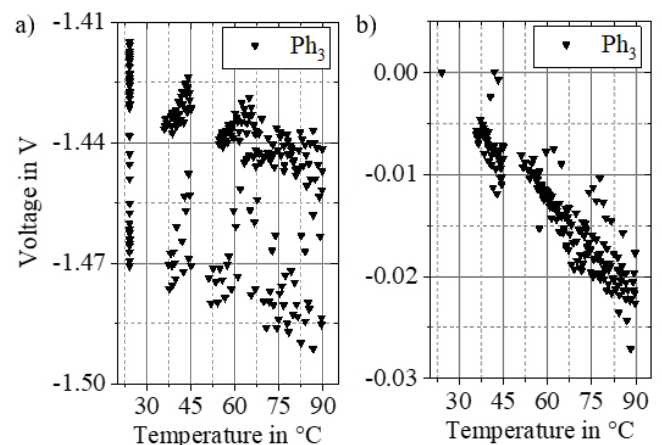


Fig. 6. The 3MA-signal "Ph<sub>3</sub>" (a) before and (b) after normalization

In Fig. 6, the data normalization procedure is illustrated with an example of signal phase 3 “Ph3”, which is a measured eddy current output of the 3MA-testing. As seen in Fig. 6b resulting normalized data only presents a dependency to workpiece temperature. Where the non-normalized data Fig. 6a shows a strong variation at room and at elevated temperatures due to the different microstructure present at the respective sections of the specimen. It must be mentioned that the normalized data at Fig. 6b has all 51 room temperature measurements overlapped at the same spot.

After the normalization procedure, the next step was to find temperature dependent 3MA-sensor data, as not all 41 measured sensor outputs need to be temperature dependent. To find the temperature dependent variables, Pearson’s correlation coefficient (PCC) between 3MA-sensor output and respective workpiece temperature during the measurement was calculated. The PCC measures the linear correlation between the respective 3MA-sensor and the temperature. A PCC of -1 and +1 would correspond to a perfect negative and positive correlation aligned on a line, respectively. As a rule of thumb, a correlation over 0.5 or under -0.5 would mean moderate correlation [18].

The following Table 3 presents 3MA sensors which showed above moderate correlation with the workpiece temperature with their respective PCC’s. Other than “ $V_{Mag}$ ” (Amplitude of the field magnetization) all 3MA parameters which presented a moderate correlation to the workpiece temperature (Re, Im, Ph, Mag) were a product of the Eddy current measurements. The Eddy current measurements are particularly important as they can be used for determining the residual stresses in case of Ti<sub>6</sub>Al<sub>4</sub>V [19] and  $\alpha'$ -martensite content in the subsurface in case of AISI 304 [16].

Table 3. Absolute PCC of 3MA-sensor outputs

PCC	0.5 – 0.6	0.6 – 0.7	0.7 – 0.8	0.8 – 0.9	0.9 – 1.0
3MA-Sensor	$V_{Mag}, Re_1$	$Im_1, Mag_1, Re_2, Im_3,$ $Ph_1, Mag_2$	$Mag_3$	$Ph_2, Im_4,$ $Mag_4$	$Re_3, Ph_3,$ $Ph_4$

To model the effect of temperature, linear regression was used on 3MA sensor outputs, whose PCC indicated a significant linear correlation. In the presented work an absolute PCC over 0.6 was considered as a significant temperature induced error for the 3MA measurement. In Fig. 7, 4 linear regression lines have been presented with the respective normalized 3MA measurements. Each illustrated sensor data covers a different range of PCC (see Table 3) to visualize the effectiveness of the method. When the performance of the respective models is compared by the R<sup>2</sup> score, the best fit was achieved for the “Ph<sub>4</sub>” which was 0.9. Sensor data “Im<sub>1</sub>” performed the worst with an R<sup>2</sup> score of 0.4. The regression lines of “Re<sub>2</sub>” and “Mag<sub>4</sub>” achieved R<sup>2</sup> scores of 0.57 and 0.67 respectively. When the R<sup>2</sup> score of the sensor data is compared to the respective PCC, it can be seen that lower R<sup>2</sup> scores are attained at sensor data which presented lower PCC meaning a worse fit. However, when looked carefully at Fig.7, the regression lines systematically overpredict the temperature influence in the range of 36 to 45 °C. As seen in Fig. 3 cooling simulation was less accurate at the temperature range and lower temperatures were simulated.

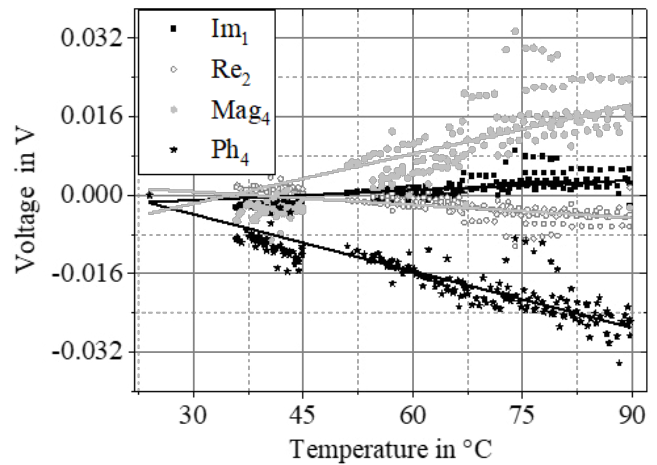


Fig. 7. Regression lines of various normalized 3MA-signal data

The linear regression performed well for 16 3MA-sensor outputs that had an absolute PCC over 0.6. The errors seen in Fig 7. at low temperatures occur as a combined result of the measurement error of the thermocouple and the simulation. As tested specimens had different tempering levels and were machined under different conditions, a minor error between the measured data and the regression line was present at all sensor outputs. Overall, the linear regression can accurately predict the temperature induced change of 3MA signals in the tested range.

At the final step, the regression lines determined from the experimental data are used to compensate the temperature induced error. At the following Fig. 8 the 3MA sensor data “Re<sub>3</sub>” has been illustrated prior (a) and after (b) the error compensation. The red, green and blue colored points represent measurements done on sections, which were machined under same conditions but with a cutting speed of 100, 200 and 300 m/min, respectively. As illustrated the linear regression-based model performed well and compensated the workpiece temperature induced error on 3MA signals. However, in the ideal case measurement points seen in Fig 8b should lie in perfect horizontal lines after error compensation, showing no variation despite increasing specimen temperature. Unfortunately, due to the measurement errors, possible differences of sensor lift-off between experiments not all data lie in a perfect line after the error compensation.

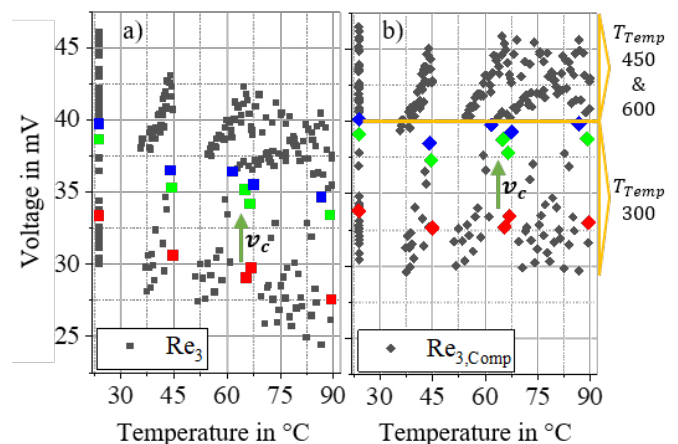


Fig. 8. The 3MA-signal “Re<sub>3</sub>” (a) before and (b) after error compensation

In Fig. 8, the real part of the Eddy current signal at 3<sup>rd</sup> frequency “Re<sub>3</sub>” varies between 46 and 30 mV at room temperature due to the different microstructure and residual stresses present at the specimen segments. The different surface properties result in 16 mV change in the “Re<sub>3</sub>” signal. Similarly, increasing the cutting speed from 100 to 300 m/min results in different surface properties which in turn would cause the sensor output “Re<sub>3</sub>” to rise about 7 mV. However, as seen in Fig. 8a when a 3MA measurement is done on a specimen at elevated temperatures (60°C) and later when at room temperature the “Re<sub>3</sub>” signal will decrease about 4 mV which would cause a significant error. Despite the broad range of cutting parameters and different tempering levels used in the experiments the error compensation is robust. In particular, compensated eddy current signal made it possible to distinguish between higher ( $T_{Temp} = 450$  &  $600$  °C) and lower ( $T_{Temp} = 300$  °C) tempering levels (see Fig. 8b).

Experiments done in Section 3.1 did not use higher depth of cut or feed rate, as flying chips interfered with the temperature measurements. In reality, machining with a higher depth of cut is plausible and can cause workpiece surface temperatures to exceed 60 °C (see Section 5.1). Therefore, modelling and compensating the errors associated with the workpiece temperature would be crucial in case of an in-process 3MA measurement. If a 3MA sensor is used for monitoring or closed loop control of a machining process where the sensor head is positioned closed to the cutting zone, surface properties will be measured with a significant error hindering proper process control. With the proposed error compensation approach, temperature induced errors will be eliminated, allowing measurement and comparison of in process captured 3MA-data and enabling in-process control of a machining process.

## 6. Conclusion and outlook

In the presented work, longitudinal-turning experiments were conducted on AISI 4140 which proved that workpiece surface temperatures during turning can exceed 60°C.

High-speed-3MA tests were done at various temperatures on specimens presenting 51 different surface properties. Significance analysis conducted on the 3MA data presented moderate correlation between 18 3MA signals and specimen temperature. The errors caused by workpiece temperature has been modelled and used for successfully compensating temperature associated errors.

Increased workpiece temperatures during machining significantly affected eddy current based measurements. However, by using the proposed approach the temperature associated errors can be compensated, enabling in process measurements near the cutting zone and allowing closed loop control of the respective machining process.

## Acknowledgements

The scientific work has been supported by the DFG within the research priority program SPP 2086 (SCHU 1010/65-2,

LA 2351/46-2, WO 903/4-2). The authors thank the DFG for the funding and intensive technical support.

## References

- [1] Stampfer, B., Böttger, D., Gauder, D., Zanger, F., Häfner, B., Straß, B., Wolter, B., Lanza, G., Schulze, V., 2020. Experimental identification of a surface integrity model for turning of AISI4140. *Procedia CIRP* 87, 83–88.
- [2] James, M.N., 2011. Residual stress influences on structural reliability. *Engineering Failure Analysis* 18 (8), 1909–1920.
- [3] Akcan, S., Shah, W.S., Moylan, S.P., Chandrasekar, S., Chhabra, P.N., Yang, H.T.Y., 2002. Formation of white layers in steels by machining and their characteristics. *Metall and Mat Trans A* 33 (4), 1245–1254.
- [4] Cappellini, C., Attanasio, A., Rotella, G., Umbrello, D., 2010. Formation of white and dark layers in hard cutting: influence of tool wear. *Int J Mater Form* 3 (S1), 455–458.
- [5] Hosseini, S.B., Klement, U., Yao, Y., Rytberg, K., 2015. Formation mechanisms of white layers induced by hard turning of AISI 52100 steel. *Acta Materialia* 89, 258–267.
- [6] Kalam, s., Azad, A., Kumar, O., Begum, V., Student, P., 2015. Elimination of White Layer formation during Hard Turning of AISI D3 Steel to improve Fatigue life. *IOSR Journal of Mechanical and Civil Engineering (IOSR-JMCE)* 12, 7–14.
- [7] Plogmeyer, M., González, G., Schulze, V., Bräuer, G., 2020. Development of thin-film based sensors for temperature and tool wear monitoring during machining. *tm - Technisches Messen* 87 (12), 768–776.
- [8] Böttger, D., Stampfer, B., Gauder, D., Lanza, G., Schulze, V., Straß, B., Wolter, B., 2021. Working point determination of 3MA micromagnetic NDT-technique for production integrated detection of white layer during turning of AISI4140. *Procedia CIRP* 101, 9–12.
- [9] Meurer, M., Tekkaya, B., Augspurger, T., Pullen, T., Schraknepper, D., Bergs, T., Münstermann, S., 2020. Cutting force based surface integrity soft-sensor when hard machining AISI 4140. *tm - Technisches Messen* 87 (11), 683–693.
- [10] Wolter, B., Gabi, Y., Conrad, C., 2019. Nondestructive Testing with 3MA—An Overview of Principles and Applications. *Applied Sciences* 9 (6), 1068.
- [11] Stephenson, D.A., Barone, M.R., Dargush, G.F., 1995. Thermal Expansion of the Workpiece in Turning. *Journal of Engineering for Industry* 117 (4), 542–550.
- [12] Trowbridge, J., McRae, A.L., 1884. The Effect of Temperature on the Magnetic Permeability of Iron and Cobalt. *Proceedings of the American Academy of Arts and Sciences* 20, 462.
- [13] Ankener, W., Böttger, D., Smaga, M., Gabi, Y., Strass, B., Wolter, B., Beck, T., 2022. Micromagnetic and Microstructural Characterization of Ferromagnetic Steels in Different Heat Treatment Conditions. *Sensors (Basel, Switzerland)* 22 (12).
- [14] Fricke, L.V., Thüerer, S.E., Jahns, M., Breidenstein, B., Maier, H.J., Barton, S., 2022. Non-destructive, Contactless and Real-Time Capable Determination of the  $\alpha'$ -Martensite Content in Modified Subsurfaces of AISI 304. *J Nondestruct Eval* 41 (4).
- [15] Harasztosi, L., Daróczy, L., Szabó, I.A., Balogh, Z., Beke, D.L., 2007. Temperature Dependence of Barkhausen Noise Parameters in Carbon Steel. *MSF* 537-538, 371–380.
- [16] Wang, Y., Meydan, T., Melikhov, Y., 2021. Quantitative Evaluation of the Effect of Temperature on Magnetic Barkhausen Noise. *Sensors (Basel, Switzerland)* 21 (3).
- [17] Kronenberg, M., 1954. *Grundzüge der Zerspanungslehre. Theorie und Praxis der Zerspanung für Bau und Betrieb von Werkzeugmaschinen.* Springer Berlin Heidelberg, Berlin, Heidelberg.
- [18] Mukaka, M.M., 2012. Statistics corner: A guide to appropriate use of correlation coefficient in medical research. *Malawi Medical Journal : The Journal of Medical Association of Malawi* 24 (3), 69–71.
- [19] Abu-Nabah, B.A., Yu, F., Hassan, W.T., Blodgett, M.P., Nagy, P.B., 2009. Eddy current residual stress profiling in surface-treated engine alloys. *Nondestructive Testing and Evaluation* 24 (1-2), 209–232.